doi:10.1017/S1431927622001787
Microsc. Microanal. 28 (Suppl 1), 2022

Single-Atom Level Determination of 3D Surface Atomic Structure via Neural Network-Assisted Atomic Electron Tomography

Juhyeok Lee[1], Chaehwa Jeong[1] and Yongsoo Yang[1*]

[1.] Department of Physics, Korea Advanced Institute of Science and Technology (KAIST), Daejeon, Korea.
* Corresponding author: yongsoo.yang@kaist.ac.kr

Functional properties of nanomaterials strongly depend on their surface atomic structures, but they often become largely different from their bulk structures, exhibiting surface reconstructions and relaxations [1-2]. However, most of the surface characterization methods are either limited to 2D measurements or not reaching to true 3D atomic-scale resolution, and single-atom level determination of the 3D surface atomic structure for general 3D nanomaterials still remains elusive. Atomic electron tomography (AET) has been developed as a powerful tool to determine the 3D atomic structure of nanomaterials at the single-atom level [3-8]. However, often due to geometrical limitations, only part of a full tomographic angular range is experimentally measurable (so-called "missing wedge" problem), which results in elongation and Fourier ringing artifacts along the direction of the missing information in the reconstructed tomogram. The missing wedge artifact negatively affects the accuracy of the 3D surface atomic structure determined from the tomogram.

We recently developed the neural network-assisted AET to retrieve the missing data and alleviate the missing wedge artifacts [9]. As shown in Fig. 1, our deep learning model was designed based on a 3D-unet structure [10]. The deep learning model was trained by imperfect 3D tomograms (suffering from the artifacts) as input and ideal 3D tomograms as ground truth. We applied the deep learning-assisted AET to experimentally determine the 3D atomic structure, using a Pt nanoparticle as a model system. The 3D tomogram of the Pt nanoparticle after applying the deep learning method showed that the undesirable artifacts are significantly reduced (see Fig. 2a-b) and the missing data is successfully retrieved (see Fig. 2c-d). From the deep learning-augmented tomogram, the 3D surface atomic structure was reliably measured. Based on the determined 3D surface atomic structure of the Pt nanoparticle, we found that <100> and <111> facets contribute differently to the surface strain, resulting in anisotropic strain distribution, while compressive support boundary effect was also observed (see Fig. 3). The capability of single-atom level surface characterization will not only deepen our understanding of the functional properties of nanomaterials but also open a new door for fine tailoring of their performance [11].

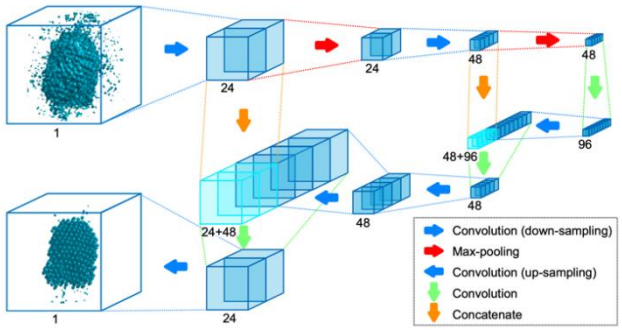

Figure 1. The framework of the deep learning model follows a 3D-unet structure. The set of boxes represents the feature map. The number of channels is denoted below each feature map.

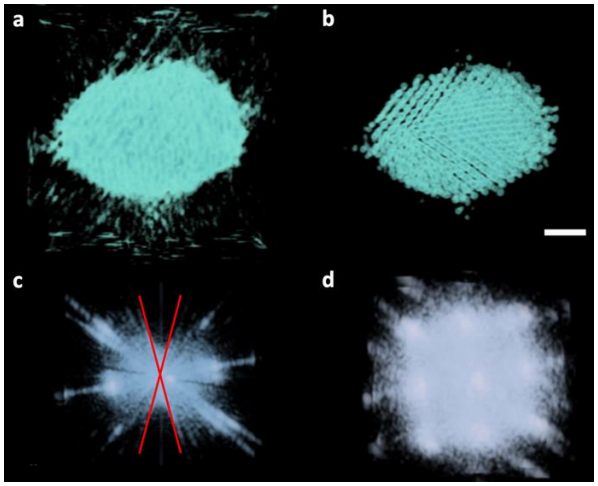

Figure 2. The 3D density map of the experimentally measured Pt nanoparticle 3D tomograms before applying the deep learning method (**a**) and after applying the method (**b**). The 3D density map of Fourier intensity of the 3D tomogram before applying the method (**c**) and after applying the method (**d**). The red lines in (**c**) are guides to visualize the missing wedge. Scale bar, 1 nm.

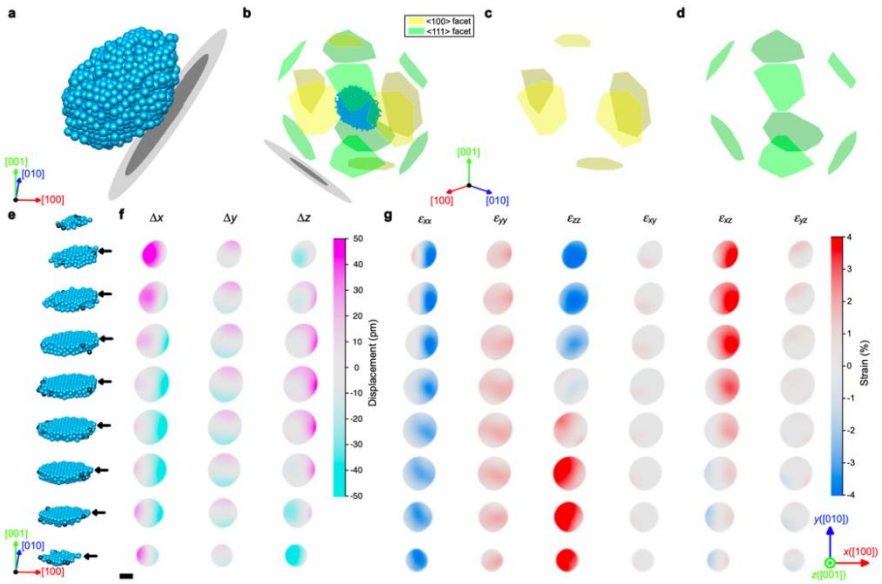

https://doi.org/10.1017/S1431927622001787 Published online by Cambridge University Press

Figure 3. a Overall atomic structure of the Pt nanoparticle with SiN substrate represented as black and gray disks. **b**–**d** Identified facet structure of the Pt nanoparticle, showing all facets (**b**), <100> facets (**c**), and <111> facets (**d**). **e** Atomic structure of the Pt nanoparticle represented in a divided into layers of one f.c.c. unit cell thickness. Blue and black atoms represent the atoms assigned and not-assigned to the ideal f.c.c. lattice sites, respectively. **f** The atomic displacements along the crystallographic axes. **g** The strain maps representing six components (ε_{xx}, ε_{yy}, ε_{zz}, ε_{xy}, ε_{xz}, ε_{yz}) of the strain tensor. The atomic displacements and strain tensors in each row were calculated from the corresponding slice pointed by the black arrows in **e**. Scale bar, 2 nm.

References:

[1] W. J. Huang et al., Nat. Mater. **7** (2008), p. 308-313.
[2] S. Van Aert et al., Nature **470** (2011), p. 374-377.
[3] R. Xu et al., Nat. Mater. **14** (2015), p. 1099–1103.
[4] Y. Yang et al., Nature **542** (2017), p. 75–79.
[5] J. Zhou et al., Nature **570** (2019), p. 500–503.
[6] X. Tian et al., Nat. Mater. **19** (2020), p. 867–878.
[7] Y. Yang et al., Nature **592** (2021), p. 60–64.
[8] J. Lee et al., Nano Lett. **22** (2022). p. 665-672.
[9] J. Lee, C. Jeong, and Y. Yang, Nature Commun. **12** (2021), 1962.
[10] Ö. Çiçek et al, Medical Image Computing and Computer-Assisted Intervention (2016), p. 424-432.
[11] We thank Chang Yun Son and Aloysius Soon for helpful discussions. This research was supported by the National Research Foundation of Korea (NRF) Grants funded by the Korean Government (MSIT) (Nos. 2019R1F1A1058236 and 2020R1C1C100623911). J.L. and C.J. were also partially supported by the KAIST-funded Global Singularity Research Program (M3I3) for 2019, 2020, and 2021. The STEM experiment was conducted using a double Cs corrected Titan cubed G2 60-300 (FEI) equipment at KAIST Analysis Center for Research Advancement (KARA). Excellent support by Hyung Bin Bae, Jin-Seok Choi, and the staff of KARA is gratefully acknowledged.